NO_x Control Options and Integration for US Coal Fired Boilers

Quarterly Progress Report

Reporting Period Start Date April 1, 2005
Reporting Period End Date: June 30, 2005

Mike Bockelie, REI
Kevin Davis, REI
Martin Denison, REI
Connie Senior, REI
Hong-Shig Shim, REI
Darren Shino, REI
Dave Swenson, REI
Larry Baxter, Brigham Young University
Calvin Bartholomew, Brigham Young University
William Hecker, Brigham Young University

July 29, 2005

DOE Cooperative Agreement No: DE-FC26-00NT40753

Reaction Engineering International
77 West 200 South, Suite 210
Salt Lake City, UT 84101

Disclaimer

Abstract

This is the twentieth Quarterly Technical Report for DOE Cooperative Agreement No: DE-FC26-00NT40753. The goal of the project is to develop cost-effective analysis tools and techniques for demonstrating and evaluating low-NO_x control strategies and their possible impact on boiler performance for boilers firing US coals. The Electric Power Research Institute (EPRI) is providing co-funding for this program. At the beginning of this quarter, the corrosion probes were removed from Gavin Station. Data analysis and preparation of the final report continued this quarter. This quarterly report includes further results from the BYU catalyst characterization lab and the in-situ FTIR lab, and includes the first results from tests run on samples cut from the commercial plate catalysts. The SCR slipstream reactor at Plant Gadsden was removed from the plant, where the total exposure time on flue gas was 350 hours. A computational framework for SCR deactivation was added to the SCR model.

Table of Contents

Experimental Methods 2
- Task 1 - Program Management 2
  - Industry Involvement 2
- Task 3 - Minimization of Impacts 2
- Task 4 - SCR Catalyst Testing 3
  - Task 4.1 Technology Assessment/Fundamental Analysis 3
  - Task 4.2 Evaluation of Commercial SCR Catalysts for Power Plant Conditions 5
  - Task 4.4 Modeling SCR Catalyst Deactivation 5

Results and Discussion 7
- Discussion of Laboratory Study of Catalyst Activity 7
  - In-situ FTIR Study 7
  - CCS Study 12
- Discussion of the SCR Model 18
  - NO_x Conversion Model 18
  - Deactivation Model 21

Conclusions 23
- Plans for Next Quarter 23

References 24

Appendix 25

1

Executive Summary

The work conducted in this project received funding from the Department of Energy under Cooperative Agreement No: DE-FC26-00NT40753. Due to the recent provision of a six-month no-cost extension, this project now has a period of performance that started February 14, 2000 and continues through September 30, 2005.

Our program contains five major technical tasks:

- evaluation of Rich Reagent Injection (RRI) for in-furnace NO_x control;
- demonstration of RRI technologies in full-scale field tests at utility boilers;
- impacts of combustion modifications (including corrosion and soot);
- ammonia adsorption / removal from fly ash; and
- SCR catalyst testing.

To date, good progress is being made on the overall program. We have seen considerable interest from industry in the program due to our successful initial field tests of the RRI technology and the corrosion monitor.

During the last three months, our accomplishments include the following:

- The electrochemical noise (ECN) corrosion probes were removed from Plant Gavin; data analysis and preparation of the final report continued this quarter.
- This quarterly report includes further results from both the BYU catalyst characterization lab and the in-situ FTIR lab and includes the first results from tests run on samples cut from the commercial plate catalysts.
    - NO_x reduction activities of two plate catalysts exposed for nominally 2063 and 3800 hours in a slipstream reactor indicated modest deactivation. Modeling of the catalytic reactions continued with an emphasis on altering the existing monolith model to describe plate systems as well.
    - Investigations of ammonia adsorption and NO reduction activity on potassium-poisoned 1% vanadia/titania catalysts indicated a decrease of ammonia adsorption and NO reduction activity upon addition of potassium. Addition of tungsten to the catalyst formulation increased ammonia adsorption on Brønsted acid sites and NO reduction activity and significantly reduced chemical poisoning of the surface.
    - Catalyst samples exposed to biomass-coal co-fired flue gases arrived in the laboratory late this quarter. Analysis of these samples continued.
- The SCR slipstream reactor at Plant Gadsden was removed, after operating for a total of 350 hours on flue gas.
- A computational framework for SCR deactivation was added to the SCR model.

Experimental Methods

Within this section we present in order, brief discussions on the different tasks that are contained within this program. For simplicity, the discussion items are presented in the order of the tasks as outlined in our original proposal.

Task 1 - Program Management

During the last performance period,

- Corrosion Probe:
  - At the beginning of this quarter, REI personnel removed the four probes from the boiler. Data analysis and preparation of the final report continued this quarter.
- SCR:
  - The SCR slipstream reactor at Plant Gadsden was removed, after operating for a total of 350 hours on flue gas.
  - This quarterly report includes further results from the BYU catalyst characterization lab and the in-situ FTIR lab, and includes the first results from tests run on samples cut from the commercial plate catalysts P1 and P2.

Industry Involvement

A technical article that will highlight the RRI NO_x control technology demonstrated earlier within this project is scheduled to be published during the next performance period in a electric utility industry trade magazine:

- "AmerenUE Sioux Plant Approaching 90% NO_x Reduction Through In-Furnace NO_x Control," to appear in Power, August, 2005.

Two presentations were made this quarter on the laboratory studies of catalyst deactivation and poisoning:

- "Poisoning/Deactivation of vanadia/titania dioxide SCR catalyst in coal and biomass fired systems", Xiaoyu Guo, Aaron Nackos, John Ashton, Larry L. Baxter, Calvin H. Bartholomew, William C. Hecker presented at the Clearwater Coal Conference, April, 19, 2005.
- "Investigation of deactivation/sulfation on vanadia/titanium dioxide catalyst", Xiaoyu Guo, Aaron Nackos, John Ashton, Larry L. Baxter, Calvin H. Bartholomew, William C. Hecker presented at the North American Catalysis Society 19th North American Meeting, May, 27, 2005.

Task 3 - Minimization of Impacts

The beginning of April was the end of the testing period for the project. Prior to a scheduled outage at Gavin (April 4th), REI personnel removed the four probes from the boiler and shipped them back to Salt Lake City. PI data have been received for 2002 through 2005 and are currently being analyzed.

Task 4 - SCR Catalyst Testing

Selective catalytic reduction (SCR) represents the only commercially proven technology capable of achieving the relatively large NO_x reductions required to comply with the latest (amended) Clean Air Act requirements. SCR systems are being installed in most large-scale utility boilers. However, most long-term experience with SCR comes from Germany and Japan and most of this is based on high-rank coal combustion. Less experience with low-rank, subbituminous coals specifically Powder River Basin coals, appears in the literature. The literature also provides essentially no US and little foreign experience with systems co-fired with biomass. The purpose of this task is to provide both laboratory and field slipstream data and analyses, including computer models that fill this information gap.

Within this task there are for principal sub-tasks:
1. technology assessment and fundamental analysis of chemical poisoning of SCR catalysts by alkali and alkaline earth materials;
2. evaluation of commercial catalysts in a continuous flow system that simulates commercial operation;
3. evaluating the effectiveness of catalyst regeneration; and
4. develop a model of deactivation of SCR catalysts suitable for use in a CFD code.

Items 1 and 3 are principally performed at Brigham Young University (BYU) under the direction of Profs. Larry Baxter, Calvin Bartholomew, and William Hecker. Methods and equipment have been described in previous technical quarterly reports. The work effort for items 2 and 4 is being performed by REI, with assistance from the University of Utah and BYU.

Task 4.1 Technology Assessment/Fundamental Analysis

ISSR Overview

The purpose of the FTIR-ISSR is to provide definitive indication of surface-active species through in-situ monitoring of infrared spectra from catalytic surfaces exposed to a variety of laboratory and field conditions. The ISSR provides in-situ transmission FTIR spectra of SO_2, NH_3, and NO_x, among other species. Adsorption and desorption behaviors of these and other species are monitored. Quantitative indications of critical parameters, including Brønsted and Lewis acidities on fresh and exposed catalysts, are included. Indications of co-adsorption of NH_3 and NO_x help elucidate mechanisms and rates of both reactions and deactivation. Much of the existing literature focuses on SCR reactions in SO_2-free environments. A significant effort in the ISSR laboratory relates to analyzing SCR reactions under coal-relevant conditions (SO_2 laden flows).

1. Most ash-derived contaminants and oxide components of the catalyst are exposed to relatively high concentrations of SO_2 under conditions where coals high in sulfur content are burned (such is the case at many utility boilers in the United States). Sulfates thus formed or deposited on the catalyst surface may profoundly affect surface acidity and hence activity (since the active sites for SCR are thought to include acid functions).

2. Most studies have been conducted either in the absence of SO_2 or under conditions and/or during short periods unfavorable for sulfate formation. Accordingly, it is questionable if these studies are relevant to "realistic" industrial conditions involving long exposures to SO_2 in the presence of water.

3. There are conflicting views in the literature as to whether vanadium species on the catalyst surface are sulfated or not.

Preparation of Doped Catalysts

Vanadia/titania catalysts were prepared in the laboratory and doped with alkali and alkaline earth metals. The objective of this study was to search for evidence of the mechanism of catalyst poisoning by alkali and alkaline earth metals by monitoring the surface adsorbed species using the in-situ FTIR during NH_3 and NO adsorption at different temperatures and on different vanadia catalysts.

Titanium dioxide (P25, Degussa), the catalyst support, was first densified by mixing with distilled water at a 1:1.75 ratio by weight, then dried at 120˚C for 24 hours, followed by calcination at 600˚C for four hours. The densified titanium dioxide was then ground with an agate mortar and pestle into a fine powder.

1% vanadia/titania catalysts were prepared using the incipient impregnation method. Ammonia metavanadate, the precursor of vanadia, was added to a warm oxalic acid solution in a stoichiometric ratio, resulting in a deep blue solution. After the precursor solution cooled down, titania powder was added and a slurry was formed, which was then dried at 120˚C overnight, followed by calcination at 600˚C for six hours. After calcination, the catalysts were ground with an agate mortar and pestle into a fine powder.

KNO_3, $NaNO_3$, and $Ca(NO_3)_2$ were used as the precursors for K, Na, and Ca, respectively. Poisoned catalysts were prepared by impregnating 1% vanadia/titania catalyst powder incipiently using the precursor solutions of K, Na, and Ca, respectively, then dried at 120˚C overnight, followed by calcination at 550˚C for six hours.

In-situ IR Adsorption Studies

To collect ammonia adsorption IR spectra, the catalyst was first exposed to 1000 ppm NH_3 in helium at 50 ˚C for one hour, followed by purging with helium for another hour at 50 ˚C to make sure no physisorbed NH_3 remained. The in-situ IR spectrum was then ready to be collected.

Tests of Commercial Plate Catalysts from REI Slipstream Reactor

The catalyst characterization system (CCS) provides capabilities for long-term catalyst exposure tests required for ascertaining deactivation rates and mechanisms and a characterization facility for samples from the slipstream reactor to determine changes in reactivity and responses to well-controlled environments. This system simulates industrial flows by providing a test gas with the following nominal composition: NO, 0.1%; NH_3, 0.1%; SO_2, 0.1%; O_2, 2%; H_2O, 10%; and He, 87.7%. Both custom and commercial catalysts are tested as fresh samples and after a variety of laboratory and field exposures under steady conditions.

The CCS quantitatively determines deactivation mechanisms by measuring specific, intrinsic catalyst reactivity of custom (laboratory) and commercial catalysts under a variety of conditions. These catalysts are impregnated with a variety of contaminants, including Ca, Na, and K. In addition, the CCS characterizes samples of catalyst from slipstream field tests to determine similar data and changes in characteristics with exposure. Advanced surface and composition analyses are used to determine composition, pore size distribution, surface area, and surface properties (acidity, extent of sulfation, etc.).

During this quarter, tests were run on samples cut from the commercial plate catalysts P1 and P2 exposed to flue gas at Rockport Unit 1. Samples from the P1 catalyst consisted of three samples taken from the fresh catalyst, three samples taken from the catalyst exposed for 2063 hours in the slipstream reactor, and six samples taken from the catalyst exposed for 3800 hours. Of the 3800-hour exposed P1 samples, three were taken from the top section of the chamber in the slipstream reactor and three were taken from the bottom section of the chamber. The P2 samples consisted of three fresh samples, three samples from the 2063-hour exposed catalyst, and three samples from the 3800-hour exposed catalyst (two of these from the top part of the chamber, 1 from the bottom). All of the samples were 3.0 cm long and 1.7 cm wide. Samples cut from the exposed catalysts were taken from the windward end of the slipstream reactor chamber.

Conditions for the tests were the same as those used to test the monolith catalysts: gas flow of 1000 sccm comprising 2% O_2, 10 % H_2O, 900 ppm NH_3, 900 ppm NO, and the balance He; temperature varied between 275 and 325 ^oC.

Task 4.2 Evaluation of Commercial SCR Catalysts for Power Plant Conditions

Biomass Co-firing Tests at Gadsden

Data from the plant PI system continued this quarter. The total exposure to flue gas in the slipstream reactor at Gadsden was about 350 hours, as shown in Figure 10. Problems with plugging of the slipstream reactor and with the remote communications limited the operation of the slipstream reactor at Gadsden. Furthermore, the boiler was not operational during all of the six-month period due to dispatch requirements and outages.

Task 4.4 Modeling SCR Catalyst Deactivation

Detailed mechanisms for reduction of NO across SCR catalysts have been developed (e.g., Ref. 1 through 4). The framework of the Chen model[1] (described in the Appendix) was adopted to understand the NO reduction using a first-order model. In the specific application of this model, REI used the mass transfer coefficient after Beeckman and Hegedus[5] for developing laminar flow in rectangular ducts. For plate catalysts, the shape factor (asymptotic Sherwood number) was taken from Ramanathan et al.[6]

This approach accounts for mass-transfer in the channel and within the porous catalyst. Previous work has shown that the NO reduction reaction is partially mass-transfer limited. For example, Dumesic et al. measured effectiveness factors for NO under industrial SCR conditions that ranged from 0.22 to 0.38.[2] Beeckman measured effective diffusion coefficients for NO within the walls of commercial SCR catalysts.[7] The effective diffusivity in the pores, D_i^e, for NO in

SCR catalyst was taken as the value measured at 300 ^{o}C[7], and then assumed to be proportional to the bulk diffusivity of NO in order to scale the diffusivity to different temperatures.

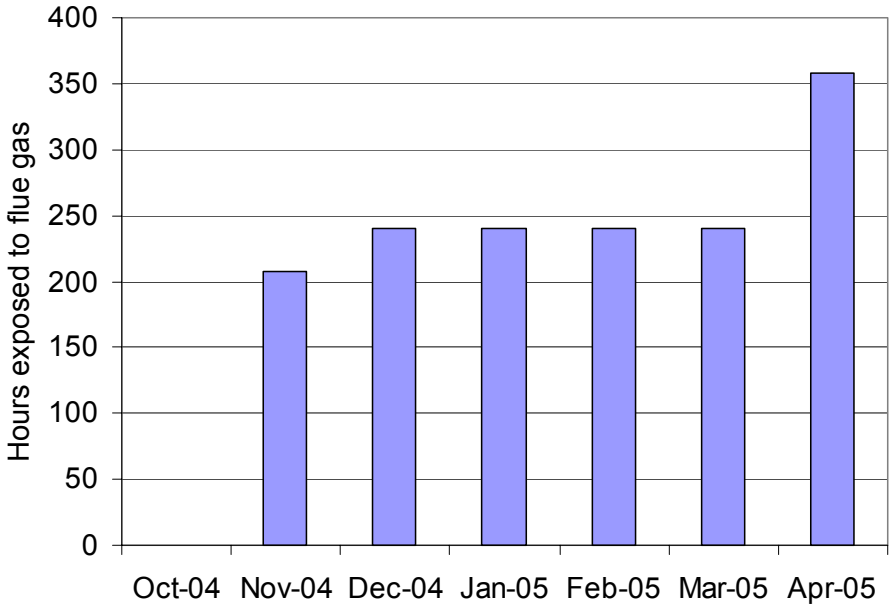

Figure 1. Exposure time of catalysts to flue gas at Plant Gadsden.

Results and Discussion

Discussion of Laboratory Study of Catalyst Activity

In-situ FTIR Study

During this quarter, NH_3 adsorption measurements were compared on 1% V_2O_5/TiO_2, 0.5 K-doped 1% V_2O_5/TiO_2, and 0.5 K-doped 1% V_2O_5 -9%WO_3/TiO_2. Figure 2 shows NH_3 adsorption on various catalysts at 50 ˚C with 1000 ppm NH_3 in the gas.

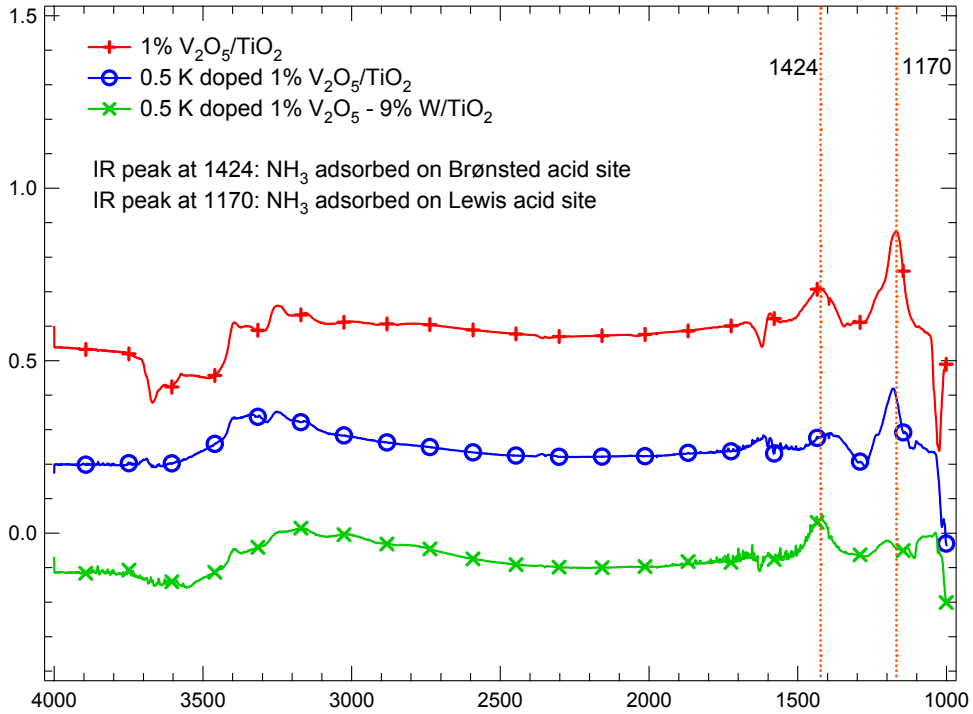

Figure 2. 1000 ppm NH_3 adsorption on 1% V_2O_5/TiO_2, 0.5 K-doped 1% V_2O_5/TiO_2, and 0.5 K-doped 1% V_2O_5 -9%WO_3/TiO_2 at 50 ˚C.

Upon NH_3 introduction, NH_3 adsorption IR peaks appeared at two regions. One group was in the low wave-number region (below 2000 cm^{-1}), which was due to the bending vibration of adsorbed NH_3 on the catalyst surface; the other group was in the high wave-number region (above 3000 cm^{-1}), which was due to the stretching vibration of adsorbed NH_3. IR peaks of NH_3 adsorption were not very easy to differentiate in the high wave-number region because peaks from NH_3 adsorption on Brønsted and Lewis acid sites overlap, but the peaks were more distinguishable in the low wave-number region. For instance, the IR peak at 1424 cm^{-1} was assigned to NH_3 adsorption on Brønsted acid sites, and the IR peak at ~1170 cm^{-1} was due to the bending

vibration of adsorbed NH_3 on Lewis acid sites. Table 1 shows the peak areas of ammonia adsorption peaks at 1424 cm^{-1} and 1170 cm^{-1} generated from various vanadia catalysts.

Table 1. NH_3 adsorption IR peak area comparison.

Catalysts	IR Peak Area	
	1424 cm^{-1}	1170 cm^{-1}
1% V_2O_5/TiO_2	10.3	22
0.5 K-doped 1% V_2O_5/TiO_2	8.6	13.3
0.5 K-doped 1% V_2O_5 -9%WO_3/TiO_2	10.8	

Comparison between 1% V_2O_5/TiO_2 and 0.5 K-doped 1% V_2O_5/TiO_2

In Figure 2, the top red line represents the IR peak of ammonia adsorbed on 1% V_2O_5/TiO_2, and the middle blue line is from NH_3 adsorption on 0.5 K-doped 1% V_2O_5/TiO_2. Apparently, the addition of potassium to the vanadia catalyst decreased the intensities of ammonia adsorption on both Brønsted and Lewis acid sites. Table 1 summarizes how the ammonia adsorption intensity, which is reflected by IR peak area, decreased by about 20% on Brønsted acid sites, and about 40% on Lewis acid sites upon potassium addition. Moreover, the IR peak around 1424 cm^{-1}, which is from ammonia adsorption on the Brønsted acid site, shifted down to a low wave-number, which indicates that potassium-addition decreased the Brønsted acid site acidity on the catalyst surface, with a negligible effect on the Lewis acid site acidity because the IR peak at 1170 cm^{-1} remained at almost the same wave number before and after addition of potassium.

Comparison between 0.5 K-doped 1% V_2O_5/TiO_2 and 0.5 K-doped 1% V_2O_5 -9%WO_3/TiO_2

Comparison of NH_3 adsorption on 0.5 K-doped 1% V_2O_5/TiO_2 catalyst (middle blue line in Figure 2) and on 0.5 K-doped 1% V_2O_5 -9%WO_3/TiO_2 catalyst (bottom green line in Figure 2) shows that upon tungsten addition, the intensity of the IR peak at 1424 cm^{-1} increased and the peak wave number shifted upward, while the intensity of the IR peak at 1170 cm^{-1} decreased largely. This shows that most of the Lewis acid sites disappeared, but both the amount and the acidity of the Brønsted acid sites increased with tungsten in the catalyst. Therefore, tungsten may remove or occupy some Lewis acid sites, and create new Brønsted acid sites on the catalyst surface. Since the wave number of the Brønsted acid sites on the 0.5 K-doped 1% V_2O_5 -9%WO_3/TiO_2 catalyst was almost the same as on the 1% V_2O_5/TiO_2 catalyst, tungsten may help to keep the Brønsted acid site acidity after the addition of potassium. An IR spectrum of ammonia adsorption on 1% V_2O_5 -9%WO_3/TiO_2 will help to elucidate the role of tungsten.

NO reduction kinetic study on K-doped catalysts

Measurement of NO reduction was conducted on K-doped vanadia catalysts with various K-to-V ratios, and the effects of both potassium and tungsten on vanadia catalyst activity for NO reduction were examined.

The first catalyst examined was 0.5 K-doped 1% V_2O_5/TiO_2 catalyst (K:V=0.5), and the corresponding NO conversions measured were zero at either 250 or 290˚C. One possible explanation for this result is that K is a very strong poison. Measurement of NO reduction was then conducted on a 0.5 Ca-doped 1% V_2O_5/TiO_2 catalyst (Ca:V=0.5), and about 5-8% NO conversion was obtained at 290 ˚C, which verifies that K is a stronger poison than Ca. Potassium is a stronger base than calcium, therefore, it is reasonable that potassium appears as a stronger poison than calcium since the active sites on vanadia catalyst are acid sites. However, results of poison studies from both our previous CCD system and literature showed that vanadia catalysts were still active for NO reduction with K:V= 0.5 on 1% V_2O_5 – 9%WO_3/TiO_2 catalyst at 300˚C. The only difference between our ISSR test and previous studies is that the catalysts tested in ISSR did not contain tungsten, while the previous results either from our CCD system or literature were based on vanadia catalyst with 9 wt% tungsten. Therefore, measurement of NO reduction was conducted on 0.5 K-doped 1% V_2O_5– 9% WO_3/TiO_2 catalyst. NO reduction was about 8% NO at 250˚C and 13% NO at 290˚C. Measurement of NO reduction was also made the on 1% V_2O_5-9%WO_3/TiO_2 catalyst at 250˚C, and an NO conversion of 42% was measured compared to an 8% NO conversion across the 1% V_2O_5/TiO_2 catalyst at 250 ˚C from previous results. Apparently, tungsten improved the catalyst activity and poisons resistance to the vanadia catalyst.

To be consistent with previous tests, where the effect of sulfation was investigated on 1% V_2O_5/TiO_2 catalysts without tungsten, K-doped 1% V_2O_5/TiO_2 catalysts with various K:V ratios of 0.3, 0.2 and 0.1 were tested to obtain NO conversions suitable for a kinetic study at a temperature range of 250-290 ˚C. The corresponding NO conversions measured are 3.92%, 7.65%, 9.68% at 290 ˚C, then 0.1 K-doped 1% V_2O_5/TiO_2 catalyst was selected to conduct a kinetic study of poisoned catalysts. Table 2 lists the catalysts that have been examined.

Table 2. Measurement of NO reduction on various K-doped vanadia catalysts

Catalysts	NO conversion	
	250 ˚C	290 ˚C
0.5 K V_2O_5/TiO_2	0	0
0.5 K 1% V_2O_5– 9% WO_3/TiO_2	8.52	12.6
1% V_2O_5– 9% WO_3/TiO_2	42.52	
0.3 K 1% V_2O_5/TiO_2		3.92
0.2 K 1% V_2O_5/TiO_2		7.65
0.1 K 1% V_2O_5/TiO_2		9.68

Details of the kinetic study have been described in the last two quarterly reports. Figure 3 shows the results of the kinetic study of NO reduction on 0.1 K-doped 1% V_2O_5/TiO_2 catalysts (bottom green line), together with previous results from sulfation studies for comparisons. Potassium addition, even a small amount (K:V =0.1), largely decreased the catalyst NO reduction activity, and the 95% confidence interval bands show that there were significant differences between fresh and poisoned 1% V_2O_5/TiO_2 catalysts. Further analyses show that the pre-exponential factor (A) of the 0.1 doped 1% V_2O_5/TiO_2 is 4,774 $cm^3/g{\cdot}s$, which is very small compared to the A value of the fresh catalyst, which is 182,003 $cm^3/g{\cdot}s$. A is an indication of the amount of the active sites, therefore, the introduction of potassium to the vanadia catalyst surface decreased the number of the active sites, or in other words, potassium poisoned the vanadia catalyst. Moreover, the activation energy (E_a) of 0.1 K-doped 1% V_2O_5/TiO_2 catalyst is 33.71 kJ/mole, which less than the activation energy of fresh 1% V_2O_5/TiO_2 catalyst of 44.92 kJ/mole. E_a variation represents changes of the reaction mechanism. Thus, the addition of potassium to the 1% V_2O_5/TiO_2 catalyst decreased the amount of the active sites, which is represented by A, and affected the reaction mechanism, reflected by a lower value of E_a.

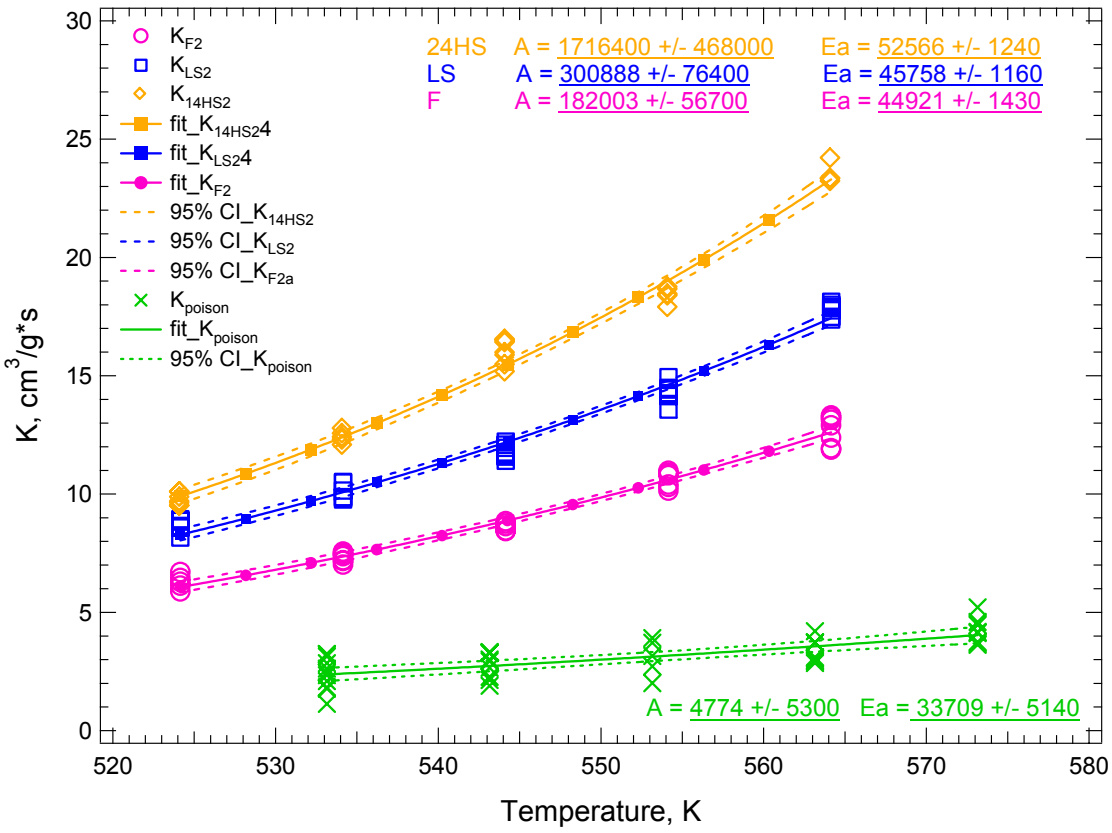

Figure 3. Catalyst activity as a function of temperature, comparison of results of poisoning studies with model predictions.

NO reduction studies on potassium-poisoned 1% V_2O_5 /TiO_2 catalysts show that vanadia catalyst lost NO reduction activity completely upon potassium addition with a K:V ratio of 0.5. Comparing the IR spectra of ammonia adsorption on 1% V_2O5/TiO_2 and 0.5 K-doped 1% V_2O_5/TiO_2 catalysts, the intensities of ammonia adsorption peaks on Brønsted and Lewis acid sites both decreased after potassium addition to the catalyst surface. Therefore, it is impossible to conclude which of the two classes of active sites were responsible for the activity loss at this point. Comparing the IR results of ammonia adsorption on the 0.5 K-doped 1% V_2O_5-9%WO_3/TiO_2 catalyst and the 0.5 K-doped 1% V_2O_5 /TiO_2 catalyst shows that addition of tungsten results in the loss of about 95% of the Lewis acid sites as illustrated in Figure 2; however, ammonia adsorption on the Brønsted acid sites remained approximately the same or even more intense compared to the ammonia adsorption on the fresh 1% V_2O_5/TiO_2, although K was present on the catalyst surface. In addition, the kinetic study showed that 0.5 K-doped 1% V_2O_5-9%WO_3/TiO_2 catalyst activity for NO reduction remained the same or even appeared higher than that of 1% V_2O_5 /TiO_2 catalyst; therefore, as long as the Brønsted acid sites remained, the NO reduction activity remained. The Lewis acid sites possessed little effect on the catalyst activity. Therefore, Brønsted acid site was more related to the NO reduction than the Lewis acid site.

In-situ FTIR studies showed that the IR peak intensity of ammonia adsorption on Brønsted acid sites from K-poisoned 1% V_2O_5/TiO_2catalysts decreased. The peak position shifted down to a

lower wave number, which indicated that K addition decreased both the number and the acidity of the Brønsted acid sites. On the other hand, the results of the NO reduction kinetic study indicated that the addition of potassium to the 1% V_2O_5/TiO_2 catalyst decreased the amount of the active sites, which is represented by a smaller A, and affected the reaction mechanism, reflected by a lower E_a. The agreement between in-situ IR analyses and the kinetic study suggests once again that the Brønsted acid sites were involve significantly in the NO reduction mechanism.

CCS Study

Activity of Commercial Plate Catalysts from REI Slipstream Reactor

Figures 4 and 5 show a comparison of NO conversion measured in the CCS for the fresh catalysts versus the exposed catalysts, for P1 and P2, respectively. The 95% confidence intervals were found by fitting the data to a second-order polynomial using Igor Pro®. In both cases, the exposed catalysts exhibited less activity than that of the fresh catalyst. The 3800-hour exposed catalysts exhibited less activity than the 2063-hour exposed catalyst.

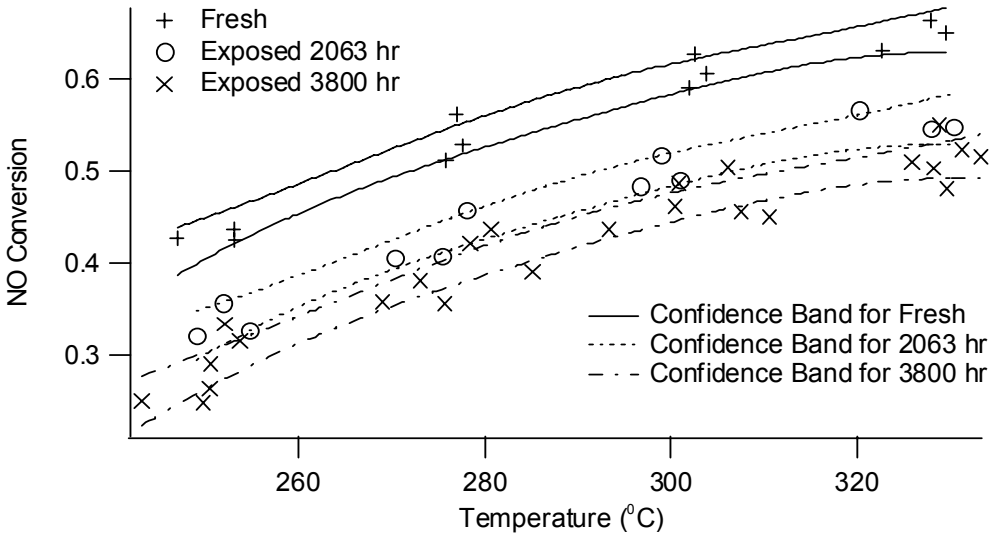

Figure 4. P1 results with 95% confidence bands

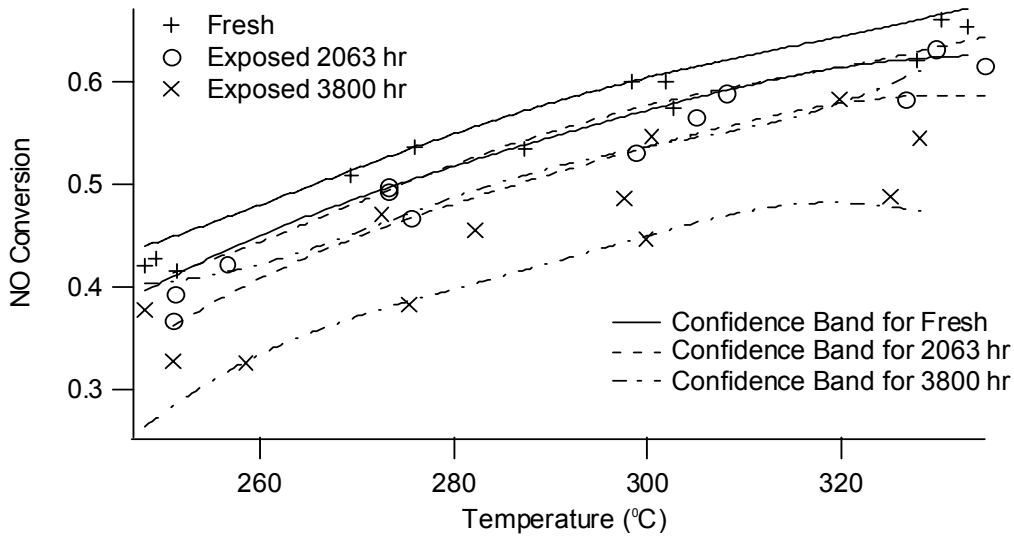

Figure 5. P2 results with 95% confidence bands.

The 3800-hour exposed P1 samples taken from the top of the slipstream-reactor chamber were compared to those taken from the bottom of the chamber. Figure 6 indicates that samples taken from both positions exhibit similar activities

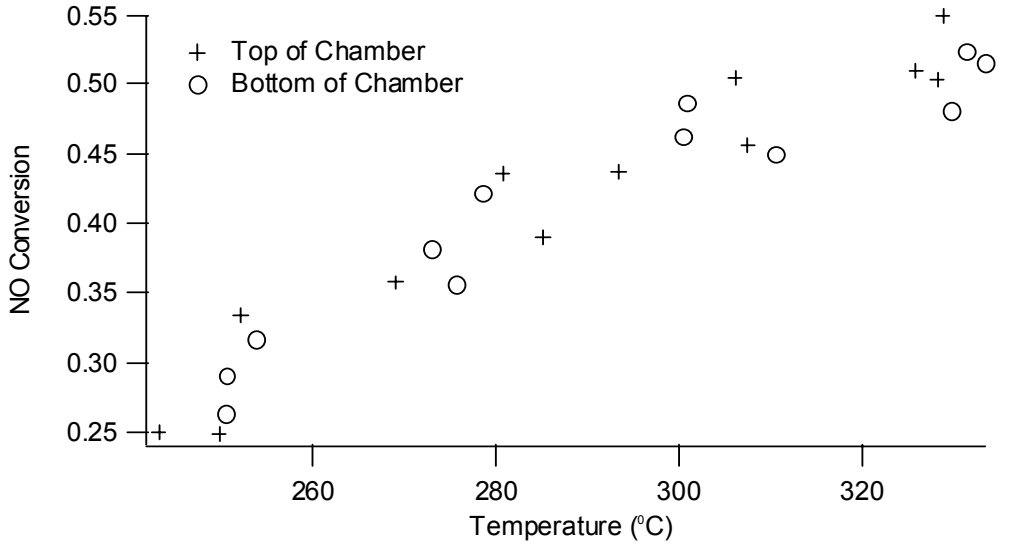

Figure 6. Top of chamber versus bottom of chamber for P1 exposed 3800 hr catalyst.

Currently, the Chen model (originally derived for monolith systems and described in the Appendix) is being examined to determine if it can be used to calculate the reaction rate constants and activation energies of the plate catalysts.[1] The Chen model may also be used to quantify the change in activity.

Reaction Rate Constant, Activation Energy, and Activity of M1 and M2 Catalysts

The Chen model (Reference 1 and Appendix), developed to describe monolith catalyst deactivation in SCR**,** provides a quantitative means of tracking deactivation and a potential means of incorporating such deactivation in a combustion simulation code. The model comparisons between the activity of the exposed catalysts and the fresh M1 and M2 catalysts appear below. The Chen model predicts NO conversion (X_{NO}) of an exposed catalyst through the equations (see subsequent section for the derivation of the Chen model):

$$X_{NO} = 1 - \exp\left(-\frac{\sigma_{cat} L}{u A_{cs}} \frac{1}{\frac{1}{k_m} - \frac{1}{(D_e k a)^{1/2}} \frac{\exp(-2\phi)+1}{\exp(-2\phi)-1}} \right) \qquad (1)$$

where

$$\phi = \left(\frac{h^2 k a}{D_e} \right)^{1/2} \qquad (2)$$

σ_{cat} = perimeter length of a monolith cell
L = monolith length
u = linear gas velocity in cell
A_{cs} = cross-sectional area of a cell
k_m = mass-transfer coefficient
D_e = effective diffusivity of NO
k = first order reaction rate constant
a = activity
Φ = Thiele modulus
h = wall half-thickness

To compare the activities, the reaction rate constants ($\underline{K}$) were found over a range of temperatures for each of the fresh catalysts by setting activity (a) equal to one. The pseudo-first-order Arrhenius' reaction rate pre-exponential factor (A) and activation energy (E_a) for each sample resulted from non-linear least-squares analyses of the measured reaction rate coefficients and temperatures. (Igor Pro® was used to fit the data):

$$k = A \exp\left(-\frac{E_a}{RT} \right) \qquad (3)$$

R = ideal gas constant
T = temperature

The results appear in Table 3 and the fit appears in Figure 7.

Table 3. k_0 and E_a Values.

Catalyst	A ($cm^3/(g*s)$)	E_a (kJ/mol)
M1	$1.06 * 10^{10}$	87.7
M2	$2.65 * 10^{10}$	97.4

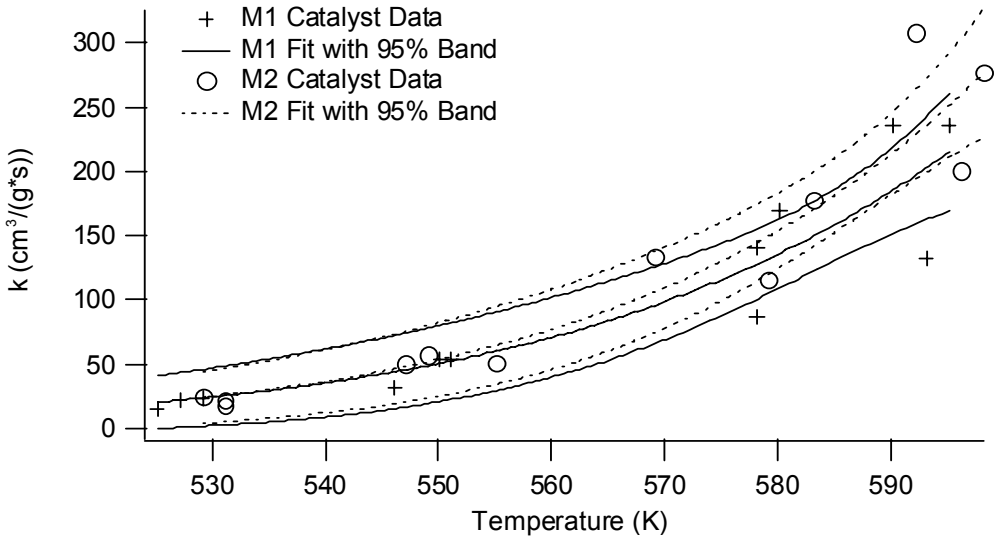

Figure 7. Arrhenius-law fit for M1 and M2.

By holding the reaction rate coefficients constant, conversion data from the exposed catalysts determine values of the activity factor (a) in the Chen model. These values appear in Table 4. Figure 8 and Figure 9 compare the Chen model fits to the actual data.

Table 4. Activity Factor Fits for Exposed Catalysts.

Catalyst	2063 hr Exposure	3800 hr Exposure
M1	1.029	1.152
M2	0.533	0.413

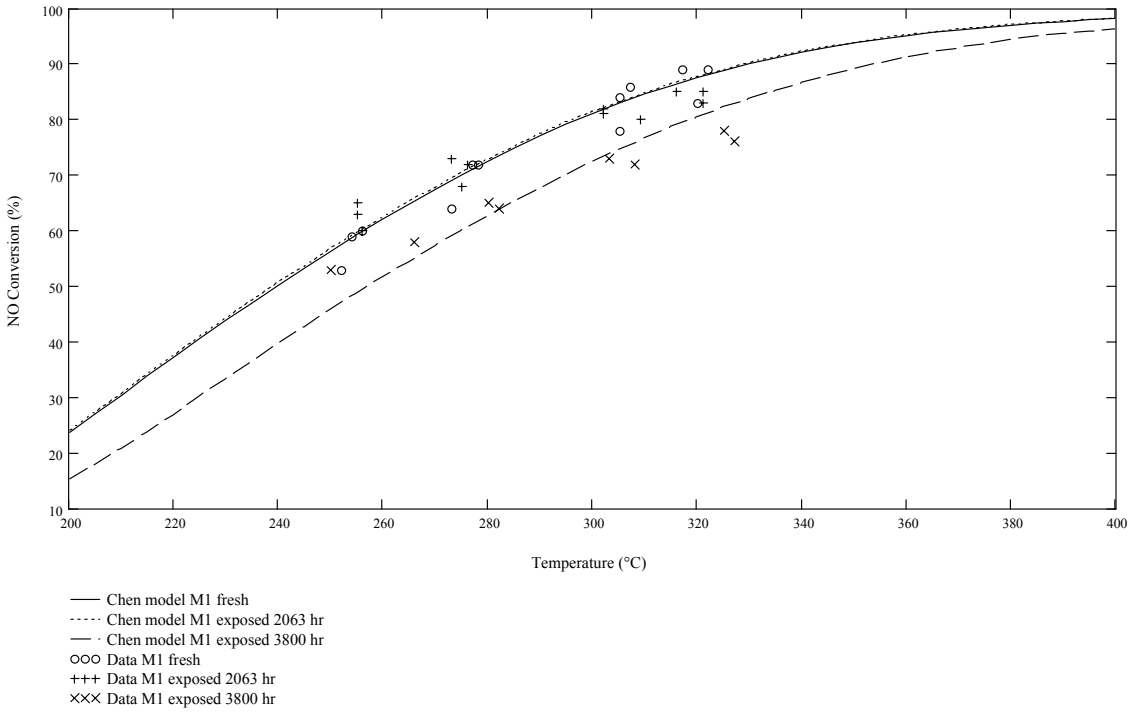

Figure 8. M1 comparison of data to Chen model prediction.

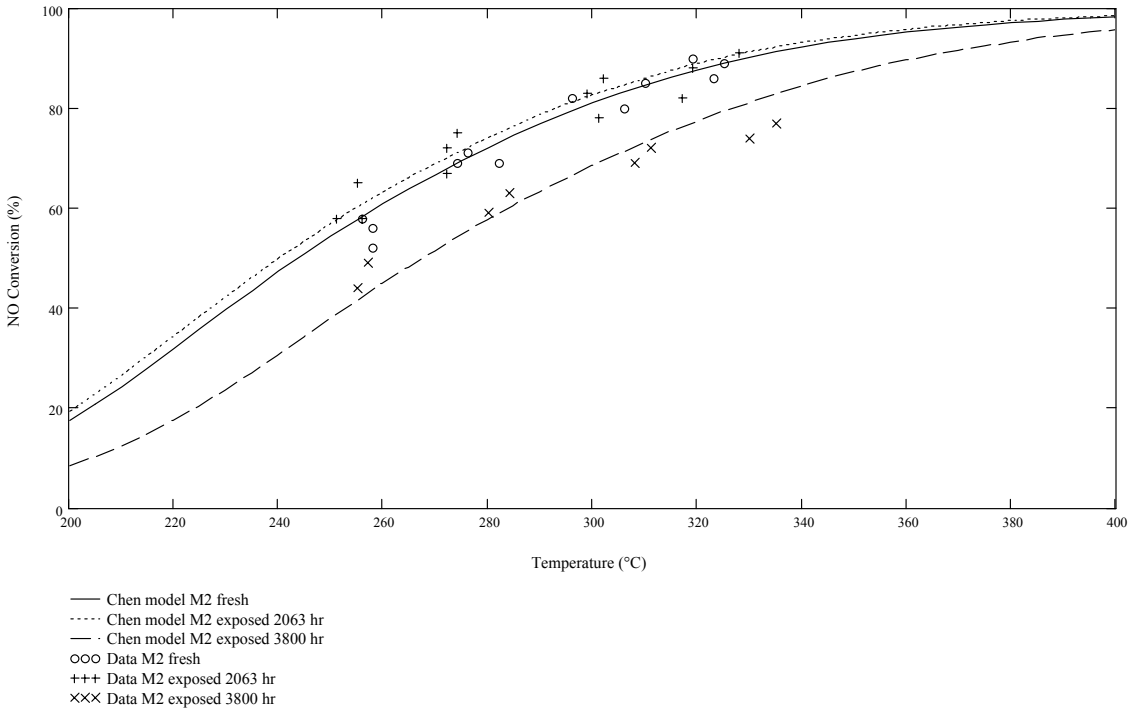

Figure 9. M1 comparison of data to Chen model prediction.

Values of the activity factor, *a*, from the Chen model, indicate that activity increases slightly after 2063 hours of exposure, presumably due to catalyst sulfation. However, after 3800 hours of exposure the activity decreases significantly. It is as yet unknown if this deactivation is caused by plugging, masking, poisoning, or a combination (Figure 10).

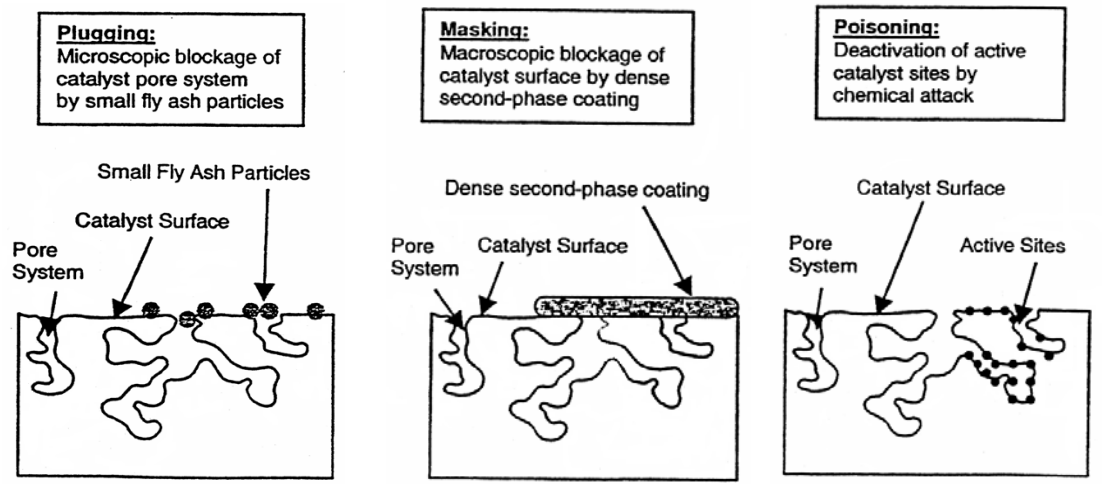

Figure 9: Comparison of Plugging, Masking and Poisoning.

Preliminary comparisons of estimated kinetic activity parameters from the field samples and the laboratory-prepared catalysts indicate that the field samples are approximately three times more active than the laboratory samples. However, these results do not account for (a) film resistance in the analysis of the field samples which is almost certainly present, (b) differences in chemical composition between the field and the laboratory samples (field samples contained tungsten whereas the lab samples with which comparisons were made did not), and (c) differences in physical structures (porosity, specific surface areas, etc.). More comparable results will be completed for the final report.

Currently, data are being collected for the M3 and BYU catalysts. Samples of the commercial catalysts that have been exposed in co-coal-biomass-combustion flue gas have been received and will be tested. The Chen model is being examined to apply it to the plate catalysts.

Discussion of the SCR Model

NO_x Conversion Model

Several sets of data of NO_x reduction for both plate and monolith catalysts were used to verify the applicability of the first-order model for SCRs in power plants.

Beeckman and Hegedus measured NO conversion in a laboratory experiment with simulated flue gas, using two commercial monolith catalysts, A and B.[5] The catalyst had the same pitch and surface area, but catalyst A had twice as much vanadia as catalyst B. The authors measured the activation energies of the two catalysts, using powdered samples, as 79.5 kJ/mole and 58.6 kJ/mole, respectively.

NO_x conversion in the monolith catalyst was measured as a function of temperature and space velocity for Catalyst A (Figure 11). NO_x conversion was predicted using an activation energy of 79.5 kJ/mole and a single pre-exponential factor. The pre-exponential factor was selected to provide the most consistent fit to the data. The pre-exponential factor is proportional to the number of active sites in the catalyst and thus will vary with the vanadium content and with the poisoning of the catalyst as it ages. The model reproduced the data well at the two highest temperatures, but not at 281°C at a high space velocity (12,000 hr^{-1}). These conditions are outside the range of typical operating conditions for SCRs in coal-fired power plants. Figure 12 shows the NO_x conversion as a function of temperature for catalysts A and B at NH_3/NO ratios of 1 and space velocities of 8,600 hr^{-1} and 6,700 hr^{-1}, respectively. The model reproduced the measured conversions well.

Previously in this program, data were taken on the slipstream reactor using a number of commercial SCR catalysts in parallel at the Rockport plant, which burned a blend of subbituminous and eastern bituminous coals as described in previous quarterly technical reports. Both monolith and plate catalysts from different manufacturers were tested in the slipstream reactor. NO_x reduction was measured across individual catalysts. Table 5 gives the parameters used in the model for these catalysts.

Table 5. Parameters in NO conversion model for commercial catalysts.

		C2 (M2)	C6 (M2)	C3 (P1)	C4 (P2)
Catalyst type		monolith	monolith	plate	monolith
Catalyst pitch	(mm)	8.2	7.4	5.7	8.2
Wall thickness	(mm)	1.3	1.3	0.9	1.3
Length	(m)	0.55	0.50	1.00	0.55
Surface area	(m^2/g)	60.0	64.5	60.0	60.0
Space velocity	(hr^{-1})	5,050	2,200-3,900	1,930-2,440	2,400-4,000
Temperature	(°C)	300-350	314-336	300-340	313-345
Inlet NO	(ppm)	310	310	310	310
Pre-exponential factor	(cm/s)	3.6E+04	7.0E+04	2.2E+01	8.5E+00
Activation energy	(kcal/mol)	58.6	58.6	58.6	58.6

Figure 13 shows a comparison of the measured and predicted NO_x reductions from the Rockport campaign in which the catalysts were new (about 300 hours of exposure to flue gas). An activation energy of 58.6 kJ/mole was used for all catalysts, with the pre-exponential factor adjusted for each catalyst.

The first-order NO_x model reproduces observed NO_x conversion from both plate and monolith catalysts in both simulated flue gas and power-plant flue gas from a slipstream reactor. The ammonia concentrations computed from the model will be used to calculate mercury oxidation.

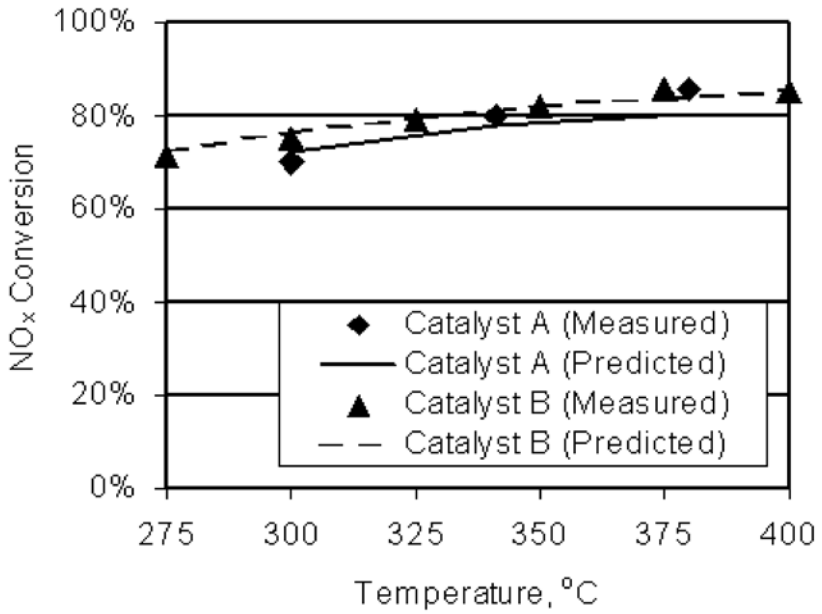

Figure 11. Measured and predicted NO_x conversion as a function of NH_3/NO ratio, temperature and space velocity for catalyst A. Data from Ref. 5.

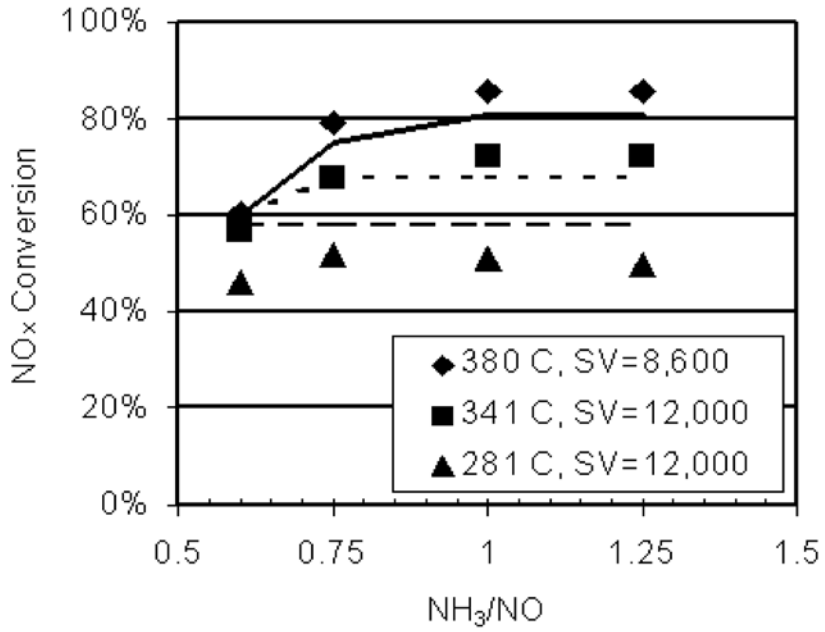

Figure 12. Measured and predicted NO_x conversion as a function of temperature at $NH_3/NO=1$. Space velocity of catalyst A is 8,600 hr^{-1} and catalyst B, 6,700 hr^{-1}. Data from Ref. 5.

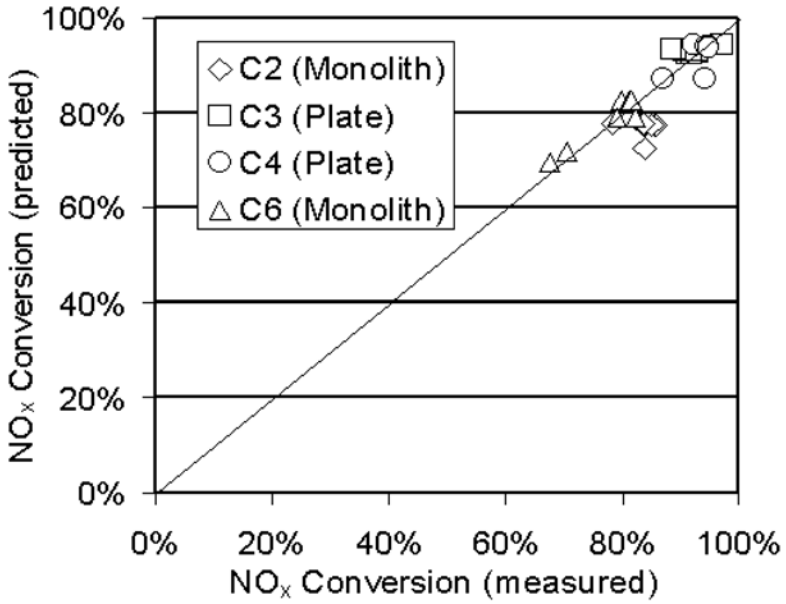

Figure 13. Measured versus predicted NO_x conversion across four different catalysts in slipstream reaction at Rockport.

Deactivation Model

Diffusion through Ash

Diffusion coefficients, D_{ash} (m^2/sec), through ash can be estimated by the correlation of Hampartsoumian et al.[8]:

$$D_{ash} = D_{AB} \cdot \theta_{ash}^{2.5}$$

θ_{ash} is the porosity of the deposited ash and will be a user input with a default value of 0.17.

Thickness of Ash Layer

The literature data are not available to develop a full correlation for ash layer thickness as a function of time in service and the channel length. For now, we will assume exponential decay of the layer thickness with increasing distance from the inlet of the channel under a given channel length (r) and a given thickness of layer at the inlet (d_i), as illustrated in Figure 14. The layer thickness at the inlet (d_i) is an input. And we will assume that the thickness of the deposited layer is zero at the outlet of the reactor channel.

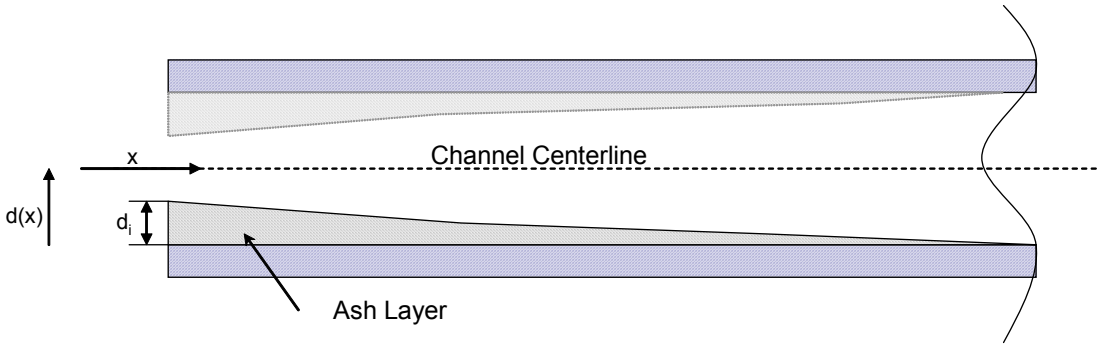

Figure 14. Sketch of the build-up of ash layer on catalyst channel.

Then, the correlation would be:

$$d(x) = \frac{\exp(-x/d_h) - \exp(-r/d_h)}{1 - \exp(-r/d_h)} \cdot d_i$$

where d(x) is the thickness of the layer (from one side only), r the whole length of the channel, d_h is the clean hydraulic diameter of the channel and d_i the initial deposit layer thickness at the inlet. Ash deposition is assumed to occur in the same way at the other side.

We can use the following correlation based on time in service (in hr) assuming a logarithmic increase of the layer thickness:

$$d_i(t) = \ln\left(\frac{e^{p/4} - 1}{t_c} \cdot t + 1\right)$$

where p is the width of the channel (m), t the time in service (hr), and t_c is the service time that needs to accumulate a thickness of p/4. t, p, and t_c are user inputs.

Then, the overall expression for d(x) would be:

$$d(x,t) = \frac{\exp(-x/d_h) - \exp(-r/d_h)}{1 - \exp(-r/d_h)} \cdot \ln\left(\frac{e^{p/4} - 1}{t_c} \cdot t + 1\right)$$

The deactivation model was run with a space velocity of 8600 hr^{-1} a temperature of 341^{o}C and a NH_3/NO ratio of 1. It was assumed that an ash thickness of 1 mm at the leading edge of the catalyst formed over 2000 hrs of service. Figure 15 shows the NO_x conversion as a function of time in service. The NO_x conversion falls from a value of 80% to 73.4% at 4000 hrs.

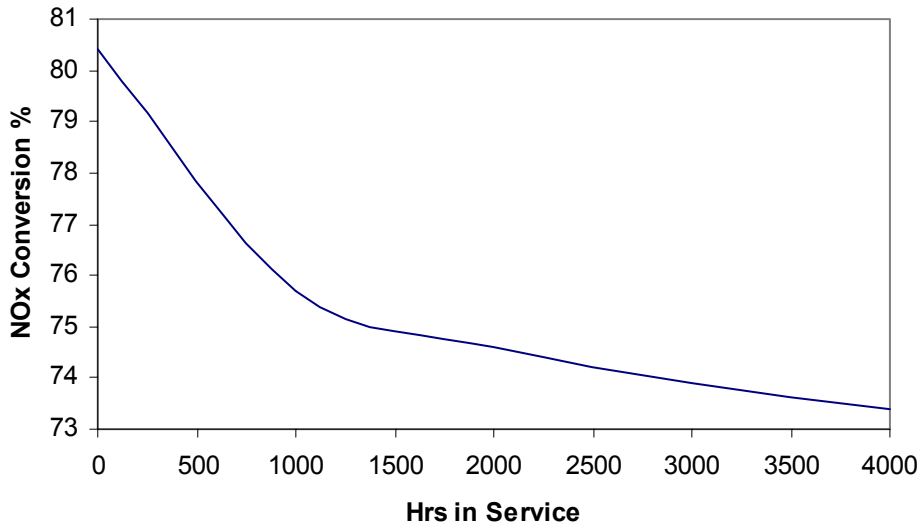

Figure 15. Calculated NO_x conversion as a function of hrs in service with a space velocity of 8600 hr^{-1} a temperature of 341 ^{o}C and a NH_3/NO ratio of 1.

23

Conclusions

Good progress has been made on several fronts during the last three months. In particular:

- The electrochemical noise (ECN) corrosion probes were removed from Plant Gavin; data analysis and preparation of the final report continued this quarter.
- This quarter, NO_x reduction activities of two plate catalysts exposed for nominally 2063 and 3800 hours in a slipstream reactor indicated modest deactivation. Modeling of the catalytic reactions continued with an emphasis on altering the existing monolith model to describe plate systems as well.
- Investigations of ammonia adsorption and NO reduction activity on potassium-poisoned 1% vanadia/titania catalysts indicated a decrease of ammonia adsorption and NO reduction activity upon addition of potassium. Addition of tungsten to the catalyst formulation increased ammonia adsorption on Brønsted acid sites, increased NO reduction activity and significantly reduced chemical poisoning of the surface.
- Catalyst samples exposed to biomass-coal co-fired flue gases arrived in the laboratory late this quarter. Analysis of these samples continued.
- The SCR slipstream reactor at Plant Gadsden was removed, after operating for a total of 350 hours on flue gas.
- A computational framework for accounting for deactivation from a porous ash layer was added to the SCR model.

Plans for Next Quarter

Corrosion probe activity for the next quarter will focus on the following:

- Complete work on final reporting requirements for the project

Activity at BYU next quarter will focus on the following:

- Analysis of slipstream SCR samples from Gadsden.

SCR slipstream activity for the next quarter will focus on the following:

- Final data analysis will be completed.

References

1. Chen, Buzanowski, Yang, and Cichanowicz. (1990). "Deactivation of the Vanadia Catalyst in the Selective Catalystic Reduction Process." Journal of the Air & Waste Management Association **40**(10):1403-1409.
2. Dumesic, J.A., Topsøe, N.-Y., Slabiak, T., Morsing, P., Clausen, B.S., Törnqvist, E., Topsøe. H. "Microkinetic Analysis of the Selective Catalytic Reduction (SCR) of Nitric Oxide over Vanadia/Titania-Based Catalysts." *New Frontiers in Catalysis* (Gucsi, L. et al., eds.), Elsevier Science Publishers, 1992.
3. Dumesic, J.A., Topsøe, N.-Y., Topsøe. H., Chen, Y., Slabiak, T. "Kinetics of Selective Catalytic Reduction of Nitric Oxide by Ammonia over Vanadia/Titania." *J. Catalysis* **1996**, *163*, 409-417.
4. Buzanowski, M.A., Yang, R.T. "Simple Design of Monolith Reactor for Selective Catalytic Reduction of NO for Power Plant Emission Control." *Ind. Eng. Chem. Res.* **1990**, *29*, 2074-2078.
5. Beeckman, J.W., Hegedus, L.L. "Design of Monolith Catalysts for Power Plant NO_x Emission Control." *Ind. Eng. Chem. Res.* **1991**, *29*, 969-978.
6. Ramanathan, K. Balakotaiah, V., West, D.H. "Bifurcation Analysis of Catalytic Monoliths with Nonuniform Catalyst Loading." *Ind. Eng. Chem. Res.* **2004**, *43*, 288-303.
7. Beeckman, J.W. "Measurement of the Effective Diffusion Coefficient of Nitrogen Monoxide through Porous Monolith-Type Ceramic Catalysts." *Ind. Eng. Chem. Res.* **1991**, *30*, 428-430.
8. Hampartsoumian, J.E., Pourkashanian, M., Williams, A, *Journal of the Institute of Energy* **1989**, March, p. 48.

25

Appendix

First-Order Model for NO Reduction

Figure A-1 schematically illustrates a two-dimensional reactor in which a reactant from the bulk flow is transported to a porous wall containing catalyst. The dimension in the direction of flow is z and the dimension perpendicular to the low is x. The origin is taken from the reactor entrance at the center of the porous catalyst. If we assume Fickian diffusion, that the catalyst is isothermal and homogeneous and that the surface reaction is first order in reactant, that the flux in the flow direction is negligible compared to the flux in the direction perpendicular to the flow, and that bulk diffusion does not influence the conversion rate, then the flux at any point in the catalyst can be equated to the rate of reaction in the catalyst as follows, where the dependence of the mole fraction of reactant on both coordinate directions is emphasized.

$$cD_e \frac{d^2y}{dx^2} = h^2 k a c y(x,z)$$

where c represents gas concentration, D_e represents the diffusivity of the reactant in the porous media, and a represents a time-dependent and dimensionless activity factor, defined as the ratio of the chemical activity in the catalyst at arbitrary time divided by its initial value. The value of a generally decreases from unity with chemical deactivation but could exceed unity because of catalyst activity increases caused, for example, by catalyst sulfation. Extensions of this model to accommodate surface fouling, bulk diffusion, and similar impacts will be discussed in the final report.

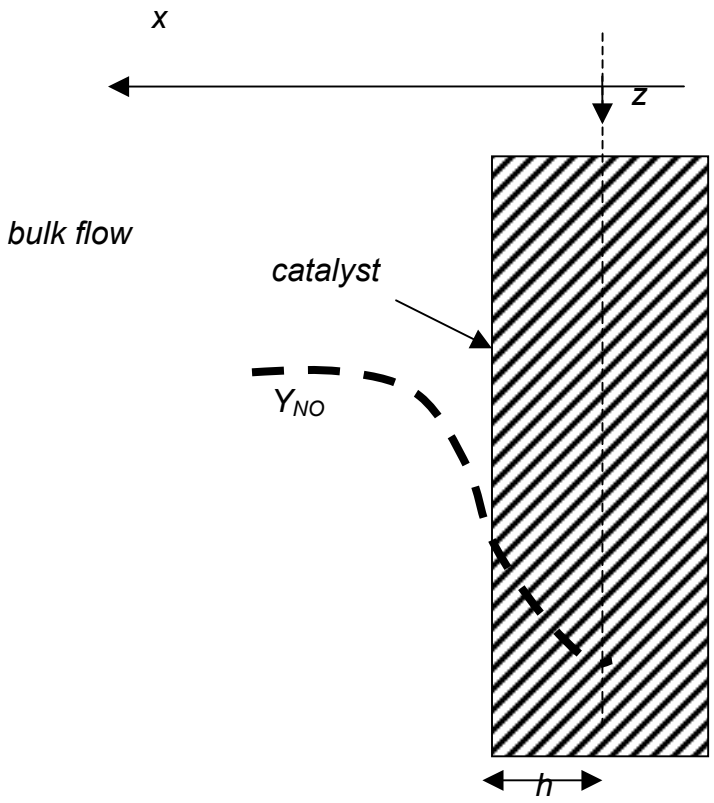

Figure A-1. Schematic diagram of a two-dimensional reactor.

This equation can be written in dimensionless form as follows:

$$\frac{d^2y'}{dx'^2} = \frac{h^2kay'}{D_e}$$

where

$$x' = \frac{x}{h}$$

and

$$y' = \frac{y_{NO}}{y^{\infty}_{NO}}$$

are based on the half-thickness of the wall (h) and the bulk mole fraction in the cell ($y\infty_{NO}$). The boundary conditions are:

$$y'\Big|_{x'=0} = 1 + Bi^{-1}\frac{dy'}{dx'}$$

$$\left.\frac{dy'}{dx'}\right|_{x'=1} = 0$$

The solution gives the concentration profile within the wall:

$$y' = \frac{e^{\phi(x'-2)} + e^{-\phi x'}}{1 - e^{-2\phi} - \frac{\phi}{Bi}\left(e^{-2\phi} - 1\right)}$$

where

$$\phi^2 = \frac{h^2ka}{D_e}$$

and

$$Bi = \frac{k_m h}{D_e}$$

This equation describes the relative impacts of film mass transfer, pore diffusion and surface reaction on conversion.

Considering the reactor, the mass balance along the axial direction of the reactor, z, is:

$$\frac{dy^{\infty}_{NO}}{dz} + \frac{k_m\sigma}{uA}\left(y^{\infty}_{NO} - y^{s}_{NO}\right) = 0$$

where u is the linear gas velocity in the cell which is assumed to be constant, σ is the perimeter length of a cell in the monolith and A is the cross-sectional area of a cell. The boundary condition is:

$$y^{\infty}_{NO}\Big|_{z=0} = y^{\infty,0}_{NO}$$

and the bulk and surface NO concentrations are related by:

$$y_{NO}^{\infty} = y_{NO}^{s}\left(1 - \frac{\phi}{Bi}\frac{e^{-2\phi}-1}{e^{-2\phi}+1}\right)$$

The overall conversion, X, of NO in the reactor at axial position L is given by:

$$X = \frac{y_{NO}^{\infty,0} - y_{NO}^{NO,L}}{y_{NO}^{\infty,0}}$$

Combining these results, the NO conversion is given by:

$$X = 1 - \exp\left[-\frac{\sigma L}{uA\left(\frac{1}{k_m} - \frac{1}{\sqrt{D_e k a}}\frac{e^{-2\phi}+1}{e^{-2\phi}-1}\right)}\right]$$